



Research Article

Enhanced Dielectric Response in PVDF-HFP-GO-Ta₂O₅ Nanocomposites: Synthesis and Characterization

Debajani Tripathy¹, Suresh Sagadevan², Wei Zhang³, Santosh K. Tiwari⁴, Srikanta Moharana^{1*}

¹School of Applied Sciences, Centurion University of Technology and Management, Odisha, India

²Nanotechnology & Catalysis Research Centre, University of Malaya, 50603 Kuala Lumpur, Malaysia

³State Key Laboratory of Structural Analysis, Optimization and CAE Software for Industrial Equipment, School of Mechanics and Aerospace Engineering, Dalian University of Technology, Dalian 116024, China

⁴Centre For New Materials & Surface Engineering, Department of Chemistry, NMAM Institute of Technology, Nitte (Deemed to be University), Nitte, 547110, India
Email: srikantanit@gmail.com

Received: 28 March 2024; **Revised:** 14 May 2024; **Accepted:** 14 May 2024

Abstract: A solution-casting approach was employed to synthesize polymer composites by incorporating tantalum pentoxide (Ta₂O₅) and graphene oxide (GO) into a PVDF-HFP (polyvinylidene fluoride-co-hexafluoropropylene) matrix. We conducted a thorough examination of the structure, morphology, and dielectric characteristics of these composites using X-ray diffraction, scanning electron microscopy, and impedance analysis. The current research showed that the composites reinforced with Ta₂O₅ in the GO-PVDF-HFP material had a consistent and noticeable look inside the PVDF-HFP matrix, suggesting effective integration. Furthermore, the relationship between the dielectric and electrical characteristics of the PVDF-HFP-GO-Ta₂O₅ composites at different weight percentages of Ta₂O₅ and frequencies has been investigated. This study revealed that the PVDF-HFP-GO-Ta₂O₅ composite films exhibited a high dielectric constant of 85, with negligible dielectric loss (< 1.5) and excellent AC conductivity (1×10^{-3}) at 102 Hz. This suggests their potential appropriateness for energy storage applications. It may offer a simple and direct way to process PVDF-HFP-GO-Ta₂O₅ nanocomposite films that have superior dielectric properties. This might enable them to be highly promising candidates for a wide range of energy storage applications.

Keywords: PVDF-HFP, graphene oxide, tantalum pentoxide, nanocomposites, dielectric properties

1. Introduction

In recent years, polymer composites (PCs) with a high dielectric constant (ϵ_r) and low dielectric loss ($\tan \delta$) have attracted academic and industrial researchers due to their wide range of potential applications, including digital memory devices, capacitors, energy storage devices, pulsed power systems, and energy harvesting [1-4]. The enhancement of polymer composites with flexibility properties, such as high strength and superior environmental resistance, is gaining interest owing to their excellent properties [5]. There are typically two methods to enhance the high dielectric constant of polymer composites: (i) using materials with high dielectric constants, such as ferroelectric ceramics or non-ferroelectric ceramics, and (ii) including conductive metals [6-9]. These approaches can be integrated to improve

the dielectric characteristics of the composites further. By incorporating conductive metals into polymer composites, a high dielectric constant can be achieved with a low volume fraction of less than 10 wt%, enhancing mechanical properties and flexibility in the final product [10]. This approach offers a more efficient and effective method for improving polymer composites than adding dielectric constant materials. Additionally, incorporating conductive metals can improve the polymer composites' electrical conductivity. This innovative method allows for a more versatile and durable final product. The study aimed to analyze how the presence of conductive fillers, such as metal particles, carbon nanotubes (CNTs), and graphene, influenced the dielectric properties of polymer PVDF composites. The researchers conducted experiments to observe the impact of these materials on the overall conductivity and performance of the composites [7-8, 11-12].

Graphene oxide is a single-atom-thick two-dimensional material composed of carbon, oxygen, and hydrogen atoms. It is derived from graphite and has unique properties, making it a promising candidate for various electronic applications [13]. However, tantalum pentoxide, often known as Ta_2O_5 , is composed of tantalum and oxygen. Due to its high dielectric constant and robust thermal stability, it is often used across several industries. Tantalum pentoxide produces optical coatings, thin film transistors, capacitors, and several other electrical components [14-15]. Ta_2O_5 is a p-type semiconductor with a cubic structure and a valence band of 3.8-5.3 eV. It has been extensively researched due to its exceptional dielectric and electrical properties [15-16]. PVDF-HFP is well recognized for its remarkable characteristics and serves as a versatile polymer material. The material exhibits significant fluorination and chemical inertness, leading to exceptional mechanical strength, remarkable chemical resistance, favorable thermal stability, and efficient membrane formation. Copolymers possess distinct attributes, including their capacity to adapt to various forms and packaging, great solubility, decreased crystallinity, remarkable electrochemical and mechanical properties, and enhanced flexibility [17-19]. For instance, Mishra and his co-workers [20] have fabricated PVDF-GO nanocomposites with dielectric constant values of up to 27.5 and comparatively lower dielectric loss values of 0.015. In the present work, we fabricated PVDF-HFP-GO- Ta_2O_5 composites containing 10 wt% GO and various weight percentages of Ta_2O_5 by a facile solution casting technique. X-ray diffraction (XRD) and scanning electron microscopy (SEM) were employed for the structural and morphological changes of the resultant PVDF-HFP-GO- Ta_2O_5 composites. The dielectric (dielectric constant and dielectric loss) and electrical (AC conductivity) of PVDF-HFP-GO- Ta_2O_5 composite films were thoroughly analyzed.

2. Experimental section

2.1 Materials

PVDF-HFP was purchased from Sigma-Aldrich in India. Its molecular weight is 180,000 g/mol. In our laboratory, we synthesized graphene oxide (GO) by modifying Hummer's method. Sodium nitrate ($NaNO_3$), potassium permanganate ($KMnO_4$), sulfuric acid (H_2SO_4), and hydrogen peroxide (H_2O_2) were the raw ingredients sourced from Himedia Pvt. Ltd. in India. Spectrochem Pvt. Ltd. supplied the sulphuric acid (H_2SO_4), N-dimethylformamide (DMF) as a solvent, and tantalum pentoxide (Ta_2O_5) as the conductive filler. All compounds were used by their respective protocols, and double-distilled water was used throughout the experiment.

2.2 Preparation of graphene oxide (GO)

Graphene oxide (GO) was successfully synthesized from purified natural graphite powder using a modified Hummer's method. This experiment involved adding graphite (1.0 g), $NaNO_3$ (0.5 g), and $KMnO_4$ (3.0 g) gradually to an ice bath, followed by spinning a 30 ml solution of H_2SO_4 . The reaction mixture was stirred at 35 °C for 1 hour, then water was added at 98 °C for 15 minutes, followed by warm water and 30% H_2O_2 for 2 hours. The resulting mixture was filtered and washed with distilled water until the supernatant reached a neutral pH. The purified sample was then dispersed in deionised water and centrifuged to yield graphene oxide.

2.3 Preparation of PVDF-HFP-Graphene Oxide- Ta_2O_5 composite films

The PVDF-HFP-GO- Ta_2O_5 composite films were synthesized by using a facile solution casting technique. First,

PVDF-HFP was dissolved in the solvent N, N-dimethylformamide (DMF) by continuous sonication and stirring to obtain the homogeneous solution. The mixture of 10 wt% GO with solvent DMF was sonicated and slowly incorporated into the prepared PVDF-HFP solution, which was stirred for 1 hour to create a uniform suspension. The PVDF-HFP-GO solution was dissolved, and then conductive Ta₂O₅ was gradually added in the desired ratios (0.3-3 wt%). A homogeneous solution was obtained from the synthesized PVDF-HFP-GO-Ta₂O₅ composites after 2.5 hours of vigorous stirring and sonication. Following vigorous stirring and sonication, the resultant solutions were transferred to a clean glass plate and dried in a vacuum oven at 75 ± 5 °C for 4 hrs to remove residual solvent. The schematic presentation of PVDF-HFP-GO-Ta₂O₅ composite films is shown in Figure 1.

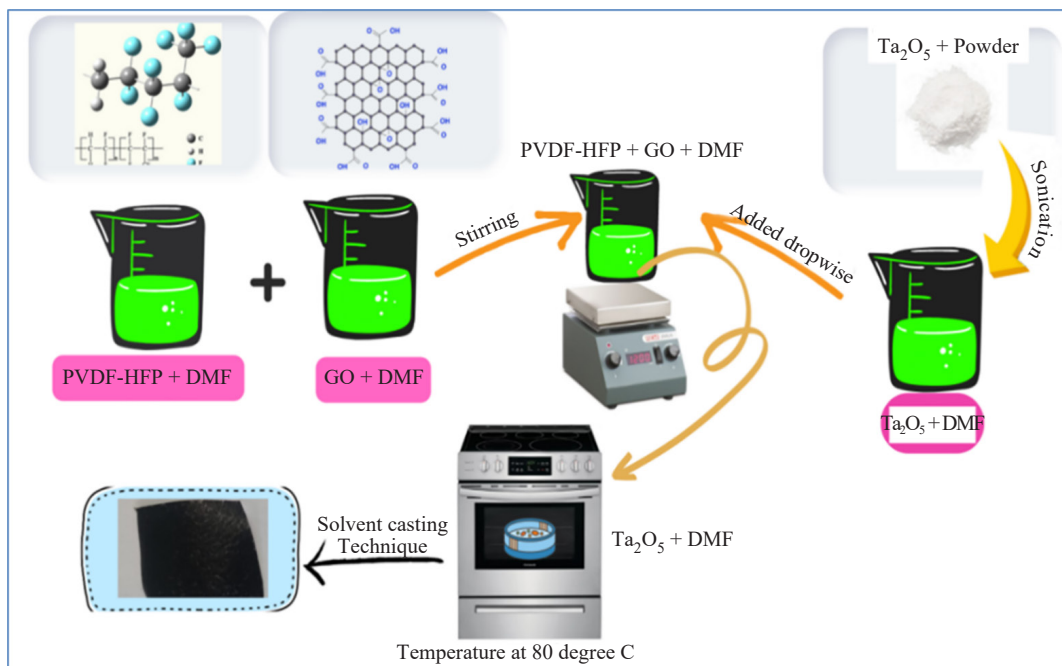


Figure 1. schematic depicting the steps involved in creating composite films of PVDF-HFP-GO-Ta₂O₅

2.4 Characterization

Utilizing an X-ray diffractometer (Rigaku Miniflex, Japan), the structure of the PVDF-HFP-GO-Ta₂O₅ composite film was explored. The PVDF-HFP-GO-Ta₂O₅ composite films were analyzed using a Bruker Vector 22 Fourier spectrophotometer, which measures infrared light in the 400-4,000 cm⁻¹ range. A surface morphology study of the generated composite films was carried out utilizing a Zeiss EVO-18 scanning electron microscope. The electrical and dielectric characteristics of the PVDF-HFP-GO-Ta₂O₅ composite films were studied at room temperature utilizing a wide frequency range (10² Hz to 10⁶ Hz) on an impedance analyzer (HIOKI 3570 Impedance analyzer).

3. Results and discussion

3.1 X-ray diffraction (XRD) analysis

Figure 2 shows the X-ray diffraction pattern of the synthesized PVDF-HFP-GO-Ta₂O₅ composite films with 0.3 wt% and 3 wt% of Ta₂O₅ contents. It clearly shows that the intensity of the peaks at 2θ corresponding to 18.5°, 20.0°, and 27.0° to the diffraction of (020), (110), and 021 crystal planes of PVDF-HFP. However, the peak at 10° corresponds to the characteristics of the carbon peak (001) for GO sheets. This indicates the presence of GO in the composite films [21-22]. When Ta₂O₅ particles are incorporated into the polymer matrix, additional diffraction peaks are observed 2θ =

22.52°, 36.24°, 46.4°, and 55.2°. These peaks correspond to the (001), (111), (002), and (2151) crystal planes of Ta₂O₅, respectively [23]. These characteristic peaks in the XRD pattern confirm the successful incorporation of GO sheets and Ta₂O₅ particles into the PVDF-HFP polymer matrix. With an increase in the concentration of Ta₂O₅ to 3 wt% compared to 0.3 wt%, more noticeable variations are seen on the XRD pattern because of the greater interactions between the Ta₂O₅ particles and polymer matrix. However, additional peaks related to PVDF-HFP and GO might potentially experience notable changes in intensity and/or location. Such alternations might indicate substantial changes in the composite's crystal structure, phase composition, and overall properties of the composite materials, potentially leading to enhanced or altered performance characteristics.

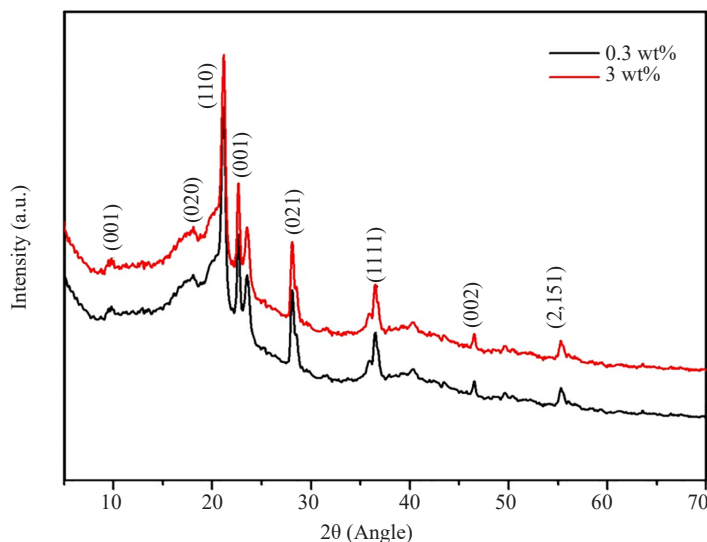


Figure 2. XRD pattern of PVDF-HFP-GO-Ta₂O₅ composite films

3.2 FTIR spectroscopy

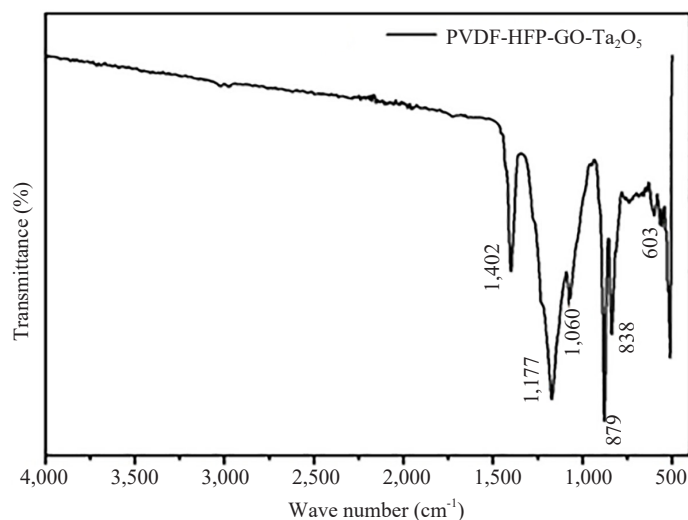


Figure 3. FTIR spectra of GO and PVDF-HFP-GO-Ta₂O₅ composite films

The FTIR spectra of PVDF-HFP-GO-Ta₂O₅ composite films are illustrated in Figure 3. It is noticed that the peak at

1,402 cm^{-1} bond is related to the C = C bond. After the incorporation of Ta_2O_5 onto the PVDF-HFP-GO nanocomposites, the corresponding peaks (1,177 and 1,060 cm^{-1}) were slightly shifted, and this may be due to the reinforcement of Ta_2O_5 into the GO sheet within the PVDF-HFP matrix [24]. In addition, the FTIR band at around 879, 838, and 603 cm^{-1} is attributed to the asymmetric stretching mode of Ta-O-Ta bonds. This peak confirms the presence of Ta_2O_5 in the GO-PVDF-HFP composite films [25].

3.3 Morphology study

The surface morphology of PVDF-HFP-GO- Ta_2O_5 composite films with a variation of Ta_2O_5 contents is shown in Figure 4(a, b). As shown in Figure 4(a), it is observed that the distribution of Ta_2O_5 particles is less homogeneous than that of the higher wt% of composite films. Also, it is noticed that Ta_2O_5 particles are warped look onto the surface of the GO sheet within the PVDF-HFP matrix. Moreover, the higher wt% (3 wt%) of Ta_2O_5 reinforced PVDF-HFP-GO composite exhibits higher dispersion and reduced agglomeration of Ta_2O_5 in the PVDF-HFP matrix, which in turn improves the interfacial attachment with an increase of dielectric constant and reduces the loss in the PVDF-HFP-GO- Ta_2O_5 nanocomposites. Further, this may also be because the polar groups of Ta_2O_5 enhance the interfacial contact between Ta_2O_5 -GO and the PVDF-HFP matrix, making the filler particles more effective. Besides, the local creation of these Ta_2O_5 -reinforced GO sheets aids in the enhancement of the nanocomposites' electrical conductivity and dielectric characteristics [26-29].

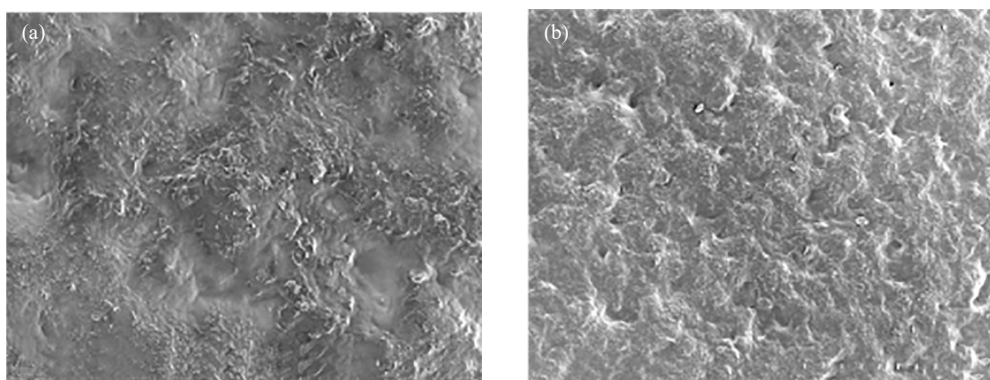


Figure 4. SEM images of (a) 0.3 wt% and (b) 3 wt% of Ta_2O_5 reinforced PVDF-HFP-GO composite films

3.4 Dielectric properties of PVDF-HFP-GO- Ta_2O_5 nanocomposites

Figure 5(a, b) shows the dielectric constant and dielectric loss of PVDF-HFP-GO- Ta_2O_5 composite films at room temperature as a function of frequency with different weight percentages of Ta_2O_5 contents. It is observed that the dielectric constant decreases with an increase in frequency when the weight % of Ta_2O_5 is increased in the lower frequency region. The dielectric constant of PVDF-HFP-GO- Ta_2O_5 hybrid films reaches a maximum of 85 at 10^2 Hz when the Ta_2O_5 contents are 3 wt%, representing a substantial improvement over the pristine PVDF-HFP matrix (~ 6). The existence of interfacial or Maxwell-Wagner-Sillars (MWS) polarization might be responsible for improving the dielectric constant of the resulting nanocomposites at low frequencies [20-21, 30-33]. The term “MWS polarisation” or “interfacial polarisation” describes the charge carriers gathered at the interface between two materials. On the other hand, when looking at frequencies greater than 10^4 Hz, the dielectric constant trend shows very little variation, especially for the weight percent (wt%) of Ta_2O_5 in the polymeric matrix (0.6, 0.9, 1 & 2 wt%). This might be because there are gaps or fractures in the nanocomposites. A higher dielectric constant results from micro-capacitor networks gradually forming in the PVDF-HFP matrix as the weight percent of conductive Ta_2O_5 filler increases. Dielectric loss is a crucial function of dielectric properties, measuring energy dissipated when an external electric field is applied. It helps estimate fillers' interface adhesion to the polymer matrix by examining the strength of dielectric loss. As Figure 5(b) demonstrates, the dielectric loss of PVDF-HFP-GO- Ta_2O_5 composite films with different weight percentages of Ta_2O_5 varies with frequency.

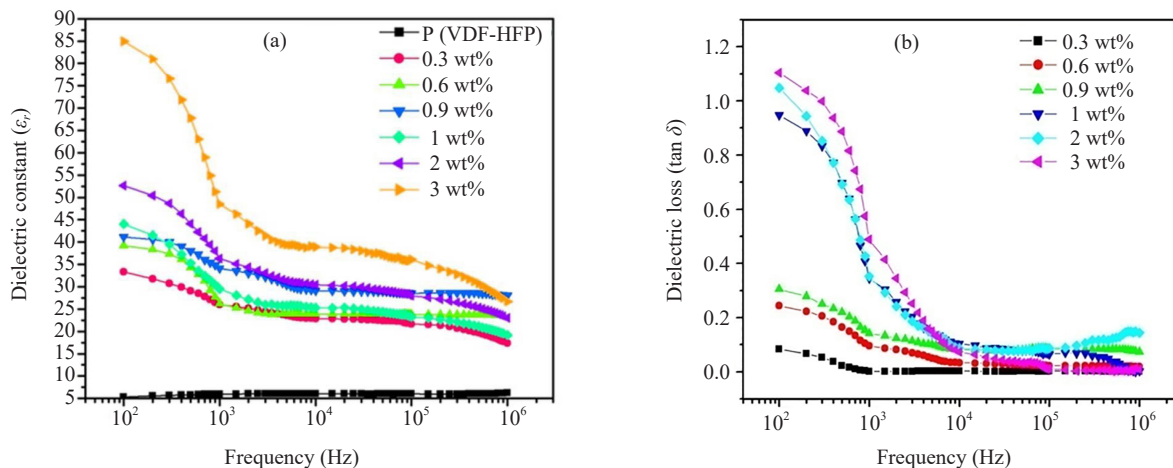


Figure 5. Frequency dependence dielectric constant (ϵ_r) (a) and dielectric loss ($\tan \delta$) (b) of PVDF-HFP-GO-Ta₂O₅ composite film

Due to interfacial polarization generated by the considerable difference in dielectric constant between the PVDF-HFP matrix and the GO fillers, there was a substantial dielectric loss in the frequency range of 1.1 to 100 Hz. The dielectric constant and dielectric loss are increased by a 3 wt% Ta₂O₅ concentration in the PVDF-HFP-GO composite film. In addition, the dielectric loss value stays low (< 1) when there is 1 wt% Ta₂O₅ in the PVDF-HFP-GO composite films. The increase in Ta₂O₅ concentration to 3 wt% leads to a rise in the dielectric loss value to 1.1. The compatibility between the GO sheet and conductive Ta₂O₅ particles in the PVDF-HFP matrix is the reason for this occurrence. The enhanced dielectric characteristics of nanocomposites may primarily be attributed to the dispersion and spatial distribution of fillers inside the polymer matrix. Thus, nanocomposites having a low dielectric loss value relative to their dielectric constant may be utilized in cutting-edge technologies such as integrated capacitors.

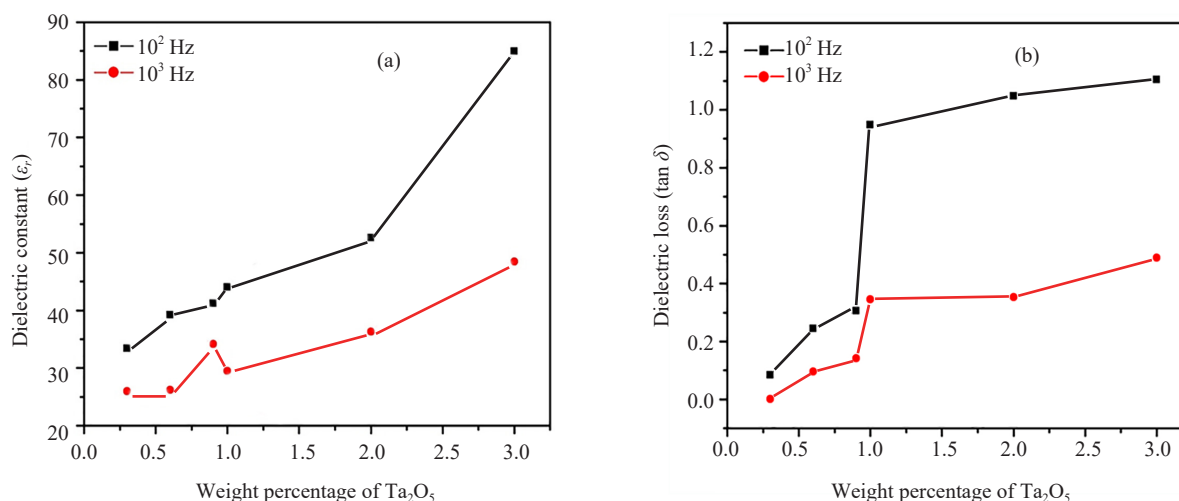


Figure 6. Dependence of dielectric constant (a) and dielectric loss (b) of PVDF-HFP-GO-Ta₂O₅ nanocomposites as a function of Ta₂O₅ contents

In Figure 6, we can see the relationship between the dielectric constant and dielectric loss at 10² Hz and 10³ Hz for PVDF-HFP-GO-Ta₂O₅ composite films with varying weight percentages of Ta₂O₅. At 10² Hz, the dielectric constant increases gradually from 0.9 wt% to 1.5 wt%, as shown in Figure 6(a). At 10³ Hz, when the filler content reaches its maximum, it rapidly climbs to 40, as seen in Figure 6(a). In particular, when the Ta₂O₅ concentration grew from 0.3 wt% to 3 wt%, the dielectric constant went up from 32 to 85 (10² Hz) and 26 to 40 (10³ Hz). The low dielectric loss ($<$

1) at 10^2 Hz and 1.2 at 10^3 Hz in PVDF-HFP-GO-Ta₂O₅ nanocomposites with different weight percent Ta₂O₅ contents could be explained by the even distribution of Ta₂O₅ particles within the GO sheet of the PVDF-HFP matrix and the reduced number of interface defects, as shown in Figure 6(b). A low-dielectric-loss composite is preferable for dielectric device applications due to its low heat output [34-35]. As the weight percentage of Ta₂O₅ was increased from 0.3 wt% to 3 wt%, the dielectric constant decreased significantly due to the growing number of defects and the higher dielectric loss.

3.5 AC conductivity study

Figure 7(a) illustrates the alternating current (AC) conductivity (AC) of PVDF-HFP-GO-Ta₂O₅ nanocomposites throughout the frequency range of 10^2 to 10^3 Hz for the Ta₂O₅ content. The nanocomposites' conductivity gradually increases from 0.3 wt% to 1 wt% as the Ta₂O₅ content increases. Subsequently, when the filler content reaches 1.4 wt%, the conductivity value experiences a significant surge, reaching 2×10^{-4} S/cm at a frequency of 10^2 Hz. On the other hand, the ac conductivity initially increases slowly and then rapidly rises from 1 wt% to 3 wt% of Ta₂O₅ contents at 10^3 Hz. However, the conductivity of PVDF-HFP-GO-Ta₂O₅ nanocomposites is dramatically enhanced by the addition of varying amounts of Ta₂O₅ (0.3 wt% to 3 wt%), indicating the existence of increased efficiency of conductive Ta₂O₅ for the development of conductive channels at the PVDF-HFP-GO interface. Moreover, the conductivity increases faster, particularly at lower frequencies, with increasing filler content.

The ac conductivity (σ_{ac}) was evaluated using the dielectric data, and an empirical equation was developed to describe the findings [36]

$$\sigma_{ac} = \omega \epsilon_r \epsilon_0 \tan \delta \quad (1)$$

Where ω is the angular frequency, ϵ_0 is the vacuum permittivity and ϵ_r is the relative dielectric constant.

The AC conductivity analysis may help better understand the frequency dependence of the electrical transport properties of PVDF-HFP-GO-Ta₂O₅ nanocomposites. The AC conductivity of Ta₂O₅ components varies positively with frequency. Figure 7(b) shows the alternating current (AC) conductivity of PVDF-HFP-GO-Ta₂O₅ composite films with varying Ta₂O₅ component percentages. It has been shown that when the proportion of Ta₂O₅ in PVDF-HFP-GO nanocomposites exceeds 3 wt%, the conducting properties of the nanocomposites exhibit substantial frequency dependency. This frequency dependency increases practically linearly with a frequency around 10^2 Hz, starting at less than 10^{-5} Scm⁻¹.

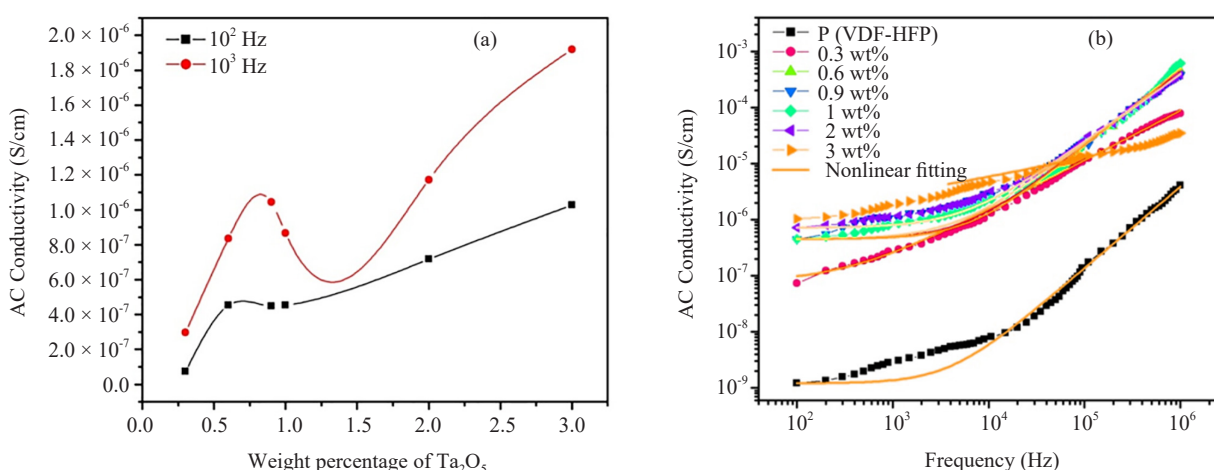


Figure 7. Dependence of AC conductivity (σ_{ac}) of the PVDF-HFP-GO-Ta₂O₅ composite films on (a) different weight percentage (wt%) of Ta₂O₅ contents with specified frequency at 10^2 - 10^3 Hz, and (b) function of frequency at room temperature

Furthermore, at all Ta₂O₅ values (0.3 wt%-3 wt%), the AC conductivity value improves with higher frequency ranges (10⁴ to 10⁶ Hz). Although linearity is a feature of insulating materials, the AC electrical conductivity of the PVDF-HFP-GO-Ta₂O₅ composite films demonstrated linearity on the log scale Figure 7(b). It was well-suited to Jonscher's universal power law. Similarly, a frequency-independent plateau region was observed in the PVDF-HFP-GO-Ta₂O₅ nanocomposites denoted as dc conductivities of 0.6 wt% to 3 wt% of Ta₂O₅ contents, and this is best characterized by the relation [37-38]:

$$\sigma_{ac} = \sigma_0 + A (\omega)^n \quad (2)$$

Where σ_0 , ω , A represents the dc conductivity, angular frequency, and pre-exponential component that varies with frequency, and n denotes a crucial exponent in the range $0 \leq n \leq 1$. This characteristic linear behavior, called a "universal dynamical response," may be seen in various conducting materials. The yellow solid line in Figure 7(b) is the fitted line, which represents the usual fit of the aforementioned equation to the experimental data. This fit demonstrates the dispersion phenomena related to Jonscher's power law. The various parameters and the values of A are shown in Table 1. This value of n is between 0.93 and 0.97. According to Jonscher [38], a relaxation phenomenon due to the mobility of charge carriers is present in any frequency-dependent conductivity.

Table 1. The fitted values of σ_0 , A, and n for PVDF-HFP-GO-Ta₂O₅ composite films

PVDF-HFP-GO-Ta ₂ O ₅ composite films	σ_0 (S/cm)	A	n	Goodness of fit (R ²)
Pristine polymer	1.2127×10^{-9}	7.0793×10^{-15}	1.456	0.992
0.3 wt%	7.3490×10^{-8}	4.0350×10^{-10}	0.889	0.994
0.6 wt%	4.53081×10^{-7}	5.12597×10^{-12}	1.321	0.995
0.9 wt%	4.47724×10^{-7}	1.24417×10^{-11}	1.251	0.993
1 wt%	4.53081×10^{-7}	2.65423×10^{-12}	1.377	0.992
2 wt%	7.17461×10^{-7}	2.00772×10^{-11}	1.215	0.995
3 wt%	1.02661×10^{-6}	1.29866×10^{-7}	0.392	0.994

4. Conclusions

The solution casting method was successfully used to fabricate composite films of Ta₂O₅-reinforced GO-PVDF-HFP. The scanning electron microscopy (SEM) analysis of PVDF-HFP-GO-Ta₂O₅ nanocomposites demonstrates that the graphene oxide (GO) and tantalum pentoxide (Ta₂O₅) particles were uniformly distributed inside the polymer matrix. The electrical and dielectric properties of PVDF-HFP-GO-Ta₂O₅ nanocomposites were tested in a wide range of frequencies from 10² Hz to 10⁶ Hz. The dielectric constant of PVDF-HFP-GO-Ta₂O₅ nanocomposites increased significantly due to the interfacial or Maxwell-Wagner-Sillars (MWS) polarisation effect. This effect is linked to the homogeneous dispersion of GO and Ta₂O₅ particles inside the polymer matrix. The dielectric constant is 85 at a filler level of 3 wt%, and dielectric loss is reduced to 1.1 at 10² Hz, about 14 times higher than pure PVDF-HFP films. This Ta₂O₅ reinforced PVDFHFP-GO composite might be a potential material for dielectric applications.

Conflict of interest

Authors declare there is no conflict of interest at any point with reference to research findings.

References

- [1] Pei JY, Yin LJ, Zhong SL, Dang ZM. Suppressing the loss of polymer-based dielectrics for high power energy storage. *Advanced Materials*. 2023; 35(3): 2203623.
- [2] Liu XJ, Zheng MS, Wang G, Zhang YY, Dang ZM, Chen G, et al. High energy density of polyimide films employing an imidization reaction kinetics strategy at elevated temperature. *Journal of Materials Chemistry A*. 2022; 10(20): 10950-10959.
- [3] Tiwari SK, Oraon R, De Adhikari A, Nayak GC. A thermomechanical study on selective dispersion and different loading of graphene oxide in polypropylene/polycarbonate blends. *Journal of Applied Polymer Science*. 2017; 134(28): 45062.
- [4] Yuan S, Shen F, Chua CK, Zhou K. Polymeric composites for powder-based additive manufacturing: Materials and applications. *Progress in Polymer Science*. 2019; 91: 141-168. Available from: doi:10.1016/j.progpolymsci.2018.11.001.
- [5] Wang D, Ren S, Chen J, Li Y, Wang Z, Xu J, et al. Healable, highly thermal conductive, flexible polymer composite with excellent mechanical properties and multiple functionalities. *Chemical Engineering Journal*. 2022; 430(4): 133163.
- [6] Golda RA, Marikani A, Alex EJ. Effect of ceramic fillers on the dielectric, ferroelectric and magnetic properties of polymer nanocomposites for flexible electronics. *Journal of Electronic Materials*. 2021; 50(6): 3652-3667.
- [7] Fang TT, Lu YC, Hsiang HI. New insight into the colossal dielectric permittivity and AC conductivity behavior of polycrystalline non-ferroelectric ceramics. *Scripta Materialia*. 2023; 223: 115104. Available from: doi:10.1016/j.scriptamat.2022.115104.
- [8] Liu L, Qu J, Gu A, Wang B. Percolative polymer composites for dielectric capacitors: a brief history, materials, and multilayer interface design. *Journal of Materials Chemistry A*. 2020; 8(36): 18515-18537.
- [9] Zhou W, Cao G, Yuan M, Zhong S, Wang Y, Liu X, et al. Core-shell engineering of conductive fillers toward enhanced dielectric properties: A universal polarization mechanism in polymer conductor composites. *Advanced Materials*. 2023; 35(2): 2207829.
- [10] He FA, Lam KH, Fan JT, Chan LW. Novel syndiotactic polystyrene/BaTiO₃-graphite nanosheets three-phase composites with high dielectric permittivity. *Polymer Testing*. 2013; 32(5): 927-931.
- [11] Yousefi N, Sun X, Lin X, Shen X, Jia J, Zhang B, et al. Highly aligned graphene/polymer nanocomposites with excellent dielectric properties for high-performance electromagnetic interference shielding. *Advanced Materials*. 2014; 26(31): 5480-5487.
- [12] Duongthipthewa A, Su Y, Zhou L. Electrical conductivity and mechanical property improvement by low-temperature carbon nanotube growth on carbon fiber fabric with nanofiller incorporation. *Composites Part B: Engineering*. 2020; 182: 107581. Available from: doi:10.1016/j.compositesb.2019.107581.
- [13] Moharana S, Mahaling RN. Silver (Ag)-Graphene oxide (GO)-Poly (vinylidene fluoride-co-hexafluoropropylene) (PVDF-HFP) nanostructured composites with high dielectric constant and low dielectric loss. *Chemical Physics Letters*. 2017; 680: 31-36. Available from: doi:10.1016/j.cplett.2017.05.018.
- [14] Mavukkandy MO, Ibrahim Y, Almarzooqi F, Naddeo V, Karanikolos GN, Alhseinat E, et al. Synthesis of polydopamine coated tungsten oxide@ poly (vinylidene fluoride-co-hexafluoropropylene) electrospun nanofibers as multifunctional membranes for water applications. *Chemical Engineering Journal*. 2022; 427: 131021. Available from: doi:10.1016/j.cej.2021.131021.
- [15] Sivaraj P, Abhilash KP, Nalini B, Perumal P, Somasundaram K, Selvin PC. Performance enhancement of PVDF/LiClO₄ based nanocomposite solid polymer electrolytes via incorporation of Li_{0.5}La_{0.5}TiO₃ nano filler for all-solid-state batteries. *Macromolecular Research*. 2020; 28: 739-750. Available from: doi:10.1007/s13233-020-8096-y.
- [16] Luo B, Wang X, Wang H, Cai Z, Li L. P (VDF-HFP)/PMMA flexible composite films with enhanced energy storage density and efficiency. *Composites Science and Technology*. 2017; 151: 94-103. Available from: doi:10.1016/j.compscitech.2017.08.013.
- [17] Fu J, Hou Y, Zheng M, Wei Q, Zhu M, Yan H. Improving dielectric properties of PVDF composites by employing surface modified strong polarized BaTiO₃ particles derived by molten salt method. *ACS Applied Materials & Interfaces*. 2015; 7(44): 24480-24491.
- [18] Yasin G, Arif M, Shakeel M, Dun Y, Zuo Y, Khan WQ, et al. Exploring the nickel-graphene nanocomposite coatings for superior corrosion resistance: manipulating the effect of deposition current density on its morphology, mechanical properties, and erosion-corrosion performance. *Advanced Engineering Materials*. 2018; 20(7): 1701166.

- [19] Nagaraju G, Karthik K, Shashank M. Ultrasound-assisted Ta₂O₅ nanoparticles and their photocatalytic and biological applications. *Microchemical Journal*. 2019; 147: 749-754. Available from: doi:10.1016/j.microc.2019.03.094.
- [20] Mishra S, Sahoo R, Unnikrishnan L, Ramadoss A, Mohanty S, Nayak SK. Investigation of the electroactive phase content and dielectric behaviour of mechanically stretched PVDF-GO and PVDF-rGO composites. *Materials Research Bulletin*. 2020; 124: 110732. Available from: doi:10.1016/j.materresbull.2019.110732.
- [21] Fu J, Hou Y, Zheng M, Wei Q, Zhu M, Yan H. Improving dielectric properties of PVDF composites by employing surface modified strong polarized BaTiO₃ particles derived by molten salt method. *ACS Applied Materials & Interfaces*. 2015; 7(44): 24480-24491.
- [22] Yasin G, Arif M, Shakeel M, Dun Y, Zuo Y, Khan WQ, et al. Exploring the nickel-graphene nanocomposite coatings for superior corrosion resistance: manipulating the effect of deposition current density on its morphology, mechanical properties, and erosion-corrosion performance. *Advanced Engineering Materials*. 2018; 20(7): 1701166.
- [23] Nagaraju G, Karthik K, Shashank M. Ultrasound-assisted Ta₂O₅ nanoparticles and their photocatalytic and biological applications. *Microchemical Journal*. 2019; 147: 749-54. Available from: doi:10.1016/j.microc.2019.03.094.
- [24] Wang D, Bao Y, Zha JW, Zhao J, Dang ZM, Hu GH. Improved dielectric properties of nanocomposites based on poly (vinylidene fluoride) and poly (vinyl alcohol)-functionalized graphene. *ACS applied materials & interfaces*. 2012; 4(11): 6273-6279.
- [25] Ono H, Koyanagi KI. Infrared absorption peak due to Ta = O bonds in Ta₂O₅ thin films. *Applied Physics Letters*. 2000; 77 (10): 1431-1433.
- [26] Xu XL, Yang CJ, Yang JH, Huang T, Zhang N, Wang Y, et al. Excellent dielectric properties of poly (vinylidene fluoride) composites based on partially reduced graphene oxide. *Composites Part B: Engineering*. 2017; 109: 91-100. Available from: doi:10.1016/j.compositesb.2016.10.056.
- [27] Li H, Chen Z, Liu L, Chen J, Jiang M, Xiong C. Poly (vinyl pyrrolidone)-coated graphene/poly (vinylidene fluoride) composite films with high dielectric permittivity and low loss. *Composites Science and Technology*. 2015; 121: 49-55. Available from: doi:10.1016/j.compscitech.2015.11.001.
- [28] Anukool W, El-Nabulsi RA, Dabagh S, Almessiere M, Ashiq MG, Guner S, et al. Effects of aluminum substitution on the microstructure and magnetic properties of cobalt ferrites prepared by the co-precipitation precursor. *Applied Physics A*. 2022; 128(8): 713.
- [29] Bouharras FE, Atlas S, Capaccioli S, Labardi M, Hajlane A, Ameduri B, et al. Synthesis and characterization of core-double-shell-structured PVDF-grafted-BaTiO₃/P(VDF-co-HFP) nanocomposite films. *Polymers*. 2023; 15(14): 3126.
- [30] Samet M, Kallel A, Serghei A. Polymer bilayers with enhanced dielectric permittivity and low dielectric losses by Maxwell-Wagner-Sillars interfacial polarization: Characteristic frequencies and scaling laws. *Journal of Applied Polymer Science*. 2019; 136(22): 47551.
- [31] Thakur A, Jangra M, Dam S, Hussain S. Enhanced dielectric constant with addition of a low amount of SnO₂ nanoparticles as fillers in a PVDF matrix with low dielectric loss. *Nano-Structures & Nano-Objects*. 2023; 34: 100978. Available from: doi:10.1016/j.nanoso.2023.100978.
- [32] Zak AK, Gan WC, Majid WA, Darroudi M, Velayutham TS. Experimental and theoretical dielectric studies of PVDF/PZT nanocomposite thin films. *Ceramics International*. 2011; 37(5): 1653-1660.
- [33] Kaur S, Singh DP. On the structural, dielectric and energy storage behaviour of PVDF-CaCu₃Ti₄O₁₂ nanocomposite films. *Materials Chemistry and Physics*. 2020; 239: 122301. Available from: doi:10.1016/j.matchemphys.2019.122301.
- [34] Nimafar M, El-Nabulsi RA, Anukool W, Haris SA, Isfahani BK, Javanifar R, et al. Characterization and biological applications of CaCO₃@Co_{0.5}Zn_{0.5}Fe₂O₄ nanoparticles. *Applied Physics A*. 2024; 130(4): 215.
- [35] Anukool W, El-Nabulsi RA, Dabagh S. Effect of Al³⁺ doping on dielectric properties of cobalt ferrite nanoparticle for using in high frequency applications. *Journal of Sol-Gel Science and Technology*. 2023; 105(2): 405-415.
- [36] Gharbi I, Oueslati A, Ates A, Mahmoud A, Zaghrioui M, Gargouri M. Investigation of structural, morphological, and electrical conductivity study for understanding transport mechanisms of perovskite CH₃NH₃HgCl₃. *RSC Advances*. 2023; 13(15): 10036-10050.
- [37] Jebli M, Albedah MA, Dhahri J, Henda MB, Bouazizi ML, Belmabrouk H. Diffuse phase transition and dielectric tunability of Ba_{0.97}La_{0.02}TiO₃ relaxor ferroelectric ceramic. *Journal of Inorganic and Organometallic Polymers and Materials*. 2022; 32(4): 1-20.

[38] Jonscher AK. The 'universal' dielectric response. *Nature*. 1977; 267(5613): 673-679.